Transverse compactlike pulse signals in a two-dimensional nonlinear electrical network

Fabien Kenmogne,[1,*] David Yemélé,[2,†] Jacques Kengne,[3,‡] and Désiré Ndjanfang[2,§]

[1]*Laboratory of Modelling and Simulation in Engineering and Biological Physics, Faculty of Science, University of Yaoundé I, Po Box 812, Yaoundé, Cameroon*

[2]*Laboratoire de Mécanique et de Modélisation des Systèmes Physiques L2MSP, Faculté des Sciences, Université de Dschang, B. P. 067, Dschang, Cameroon*

[3]*Laboratoire d' Automatique et Informatique Apliquée (LAIA), IUT-FV Bandjoun, University of Dschang, Cameroon*

(Received 2 March 2014; published 24 November 2014)

We investigate the compactlike pulse signal propagation in a two-dimensional nonlinear electrical transmission network with the intersite circuit elements (both in the propagation and transverse directions) acting as nonlinear resistances. Model equations for the circuit are derived and can reduce from the continuum limit approximation to a two-dimensional nonlinear Burgers equation governing the propagation of the small amplitude signals in the network. This equation has only the mass as conserved quantity and can admit as solutions cusp and compactlike pulse solitary waves, with width independent of the amplitude, according to the sign of the product of its nonlinearity coefficients. In particular, we show that only the compactlike pulse signal may propagate depending on the choice of the realistic physical parameters of the network, and next we study the dissipative effects on the pulse dynamics. The exactness of the analytical analysis is confirmed by numerical simulations which show a good agreement with results predicted by the Rosenau and Hyman $K(2,2)$ equation.

DOI: 10.1103/PhysRevE.90.052921 PACS number(s): 05.45.Yv, 84.40.Az, 41.20.−q

I. INTRODUCTION

Over the years, solitons have been the focal point of intense investigations in several physical branches including Bose-Einstein condensates [1], nonlinear optics [2], and nonlinear electrical lattices [3] through their dynamical equations, which requires usually a fine balance between nonlinearity and dispersion. Among the equations admitting solitary wave as solution, there is the Korteweg–de Vries (KdV) equation admitting pulse soliton as solution, which can propagate over long distance maintaining its characteristics namely the shape and the speed, and conserve these properties even after multiple collisions with other solitons. Observing the real phenomena in nature, we can realize that stationary and dynamical patterns are usually finite in extent although most equations that admit solitary wave yield solutions that are infinite in extent and which can cause long-distance interaction. To solve the adequacy problem of soliton with natural phenomena, Rosenau and Hyman [4] generalizing the KdV equation found in 1993 a new class of solitary wave which is localized in a finite region of space and requires a balance between the standard nonlinearity and nonlinear dispersion, which as solitons can survey collisions and had been named compactons.

Since this pioneering work of Rosenau and Hyman, compactons have been studied in diverse physical systems in order to put forward this new concept. We can mention the analysis of patterns on liquid surfaces [5], the nonlinear dynamics of surface internal waves in a stratified ocean under the Earth's rotation [6], the modeling of DNA opening with 1D Hamiltonian lattice [7], the dynamics of a chain of autonomous, self-sustained, dispersively coupled oscillators [8,9], the motion of melt in the Earth [10,11]; all these studies were performed by means of the compacton concept. On the same pathway, multidimensional continuum model (including two and three dimensions) of the Rosenau compacton was proposed by Rosenau, Hyman, and Staley in 2007 [12]. Another interesting application of compactons is whether they can be supported by real systems such as nonlinear electrical transmission lines (NLTLs).

NLTLs have been intensively investigated during the past few decades to produce localized solitons in both one and two spatial dimensions [13]. Several investigations have been done for managing dispersion [14,15] and for introducing nonlinearity to develop times-invariant envelope pulses [16,17]. In particular, the two-dimensional NLTLs have been studied and they exhibit extraordinary refractive properties [13,18]. It has been demonstrated that the nonlinear uniform electrical line can be used: for extremely wide band signal shaping applications [19], for waveform equalizer in the compensation scheme for signal distortion caused by optical fiber polarization dispersion mode [20], for doubling repetition rate of incident pulse streams [21], and in the scheme for controlling the amplitude (amplification) and the delay of ultrashort pulses through the coupled propagation of the solitonic and dispersive parts, which is important in that it enables the characterization of high-speed electronic devices and raises the possibility of establishing future ultrahigh signal processing technology [22]. The emergence of compactons in NLTLs can improve considerably the practical results concerning the distortionless signal in ultrahigh-speed signal processing tools and in electronic devices where they may be used to codify data [23]. Recently, Compte and Marquié [24] have outlined that when the nonlinear resistances are introduced in their series branches, NLTLs modeling the front propagation in reaction-diffusion equations can lead to the compactification

*Corresponding author: kenfabien@yahoo.fr
†dyemele@yahoo.fr
‡kengnemozart@yahoo.fr
§ndjanfang@yahoo.fr

of kink solitary waves. Since these pioneering works of Compte and Marquié, other works on compactons have followed in NLTLs. To name just few examples, Yemélé and Kenmogne [25,26] have demonstrated that if the nonlinear capacitors are introduced in the series branches of NLTL, it may exhibit dynamics compact dark solitary wave, while very recently, Ndjanfang and co-workers [27] pointed out that the NLTL with nonlinear resistances in their series branches can be interpreted by the nonlinear diffusive Burgers (NLDB) equation which can admit the traveling pulse solitary wave with compact support.

Our purpose of this work is to show that compactlike pulse signals can propagate in the two-dimensional electrical network with well-defined basic characteristics and also in the two-dimensional continuum limit. To this end, the structure of the paper is as follows. In Sec. II, we present the basic characteristics of the electrical network under consideration and derive the discrete equations governing the dynamics of signal voltage in the network. In Sec. III we focus on deriving the two-dimensional NLDB equation governing small amplitude signal in the network. In Sec. IV, exact analytical expressions of solutions, which include the cusp and the compactlike pulse solutions of the system, are obtained, and the dissipative effects of the network on the pulse motion is analyzed by means of the two-dimensional NLDB equation and the simple perturbation theory. Numerical investigations are performed in Sec. V in order to verify the validity of the theoretical prediction of the propagation of two-dimensional compactlike pulse solitary waves. Finally, in Sec. VI, concluding remarks are presented.

II. MODEL DESCRIPTION AND FUNDAMENTAL PROPERTIES OF THE TWO-DIMENSIONAL ELECTRICAL NETWORK

We consider a two-dimensional electrical network which consists of the number of identical cells connected as illustrated in Fig. 1. The nodes of the network are labeled with two discrete coordinates n and m, where n specifies the nodes in the propagation direction of the signal, while m labels the nodes in the transverse direction. In each unit cell, L_1 and NLR_1 are respectively the inductance and the nonlinear resistance in the direction of propagation (that is in n direction), while L_2 and NLR_2 are the inductance and the nonlinear resistance in transverse (or m) direction. The standard nonlinearity is introduced in the network by varicap diodes whose capacitances vary with applied voltages. Denoting by $Q_{n,m}(t)$ the nonlinear electrical charge at the (n,m)th node and by $V_{n,m}(t)$ the corresponding voltage, we assume that the charge has a voltage dependence similar to the one of an electrical Toda lattice [28]

$$Q_{n,m} = C_0 V_0 \ln(1 + V_{n,m}/V_0), \tag{1}$$

where C_0 and V_0 are constants characterizing the operating point. The nonlinear resistances (NLRs) under consideration are the standard diodes with the following current-voltage characteristics

$$i = I_0(\exp(\delta V/V_T) - 1), \tag{2}$$

where δV is the voltage difference across the nonlinear resistance, $V_T = k_B T/|q|$ is the thermal voltage, k_B is the

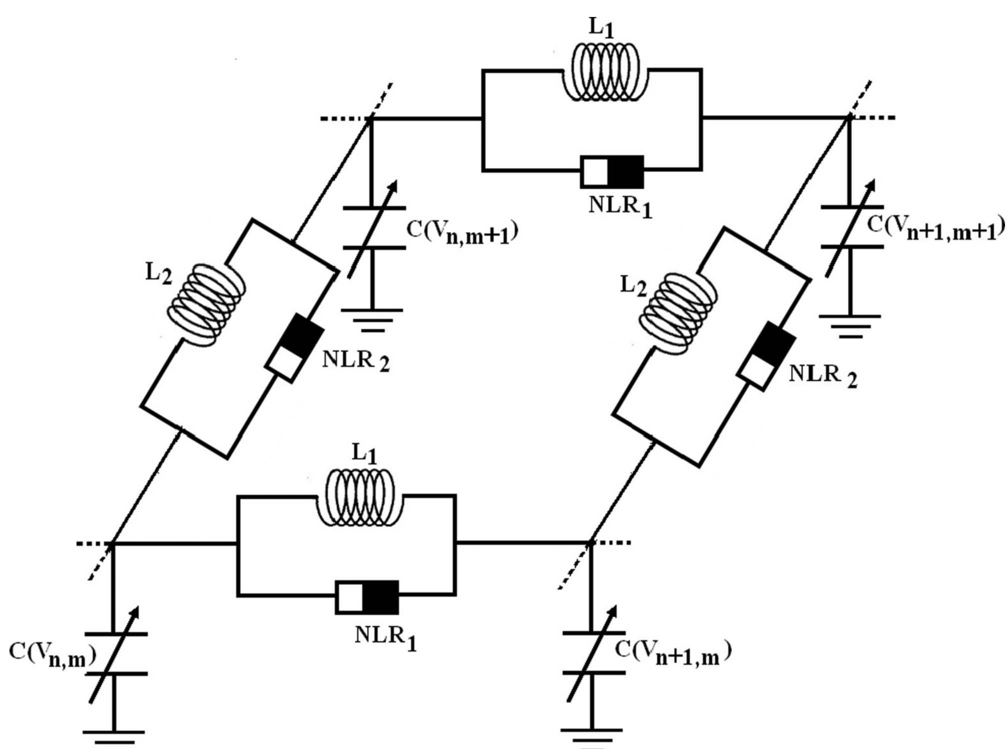

FIG. 1. Schematic representation of the two-dimensional nonlinear transmission network. Each cell contains the nonlinear capacitor $C(V)$ in the shunt branch which induces the standard nonlinearity, while in the series propagation and transverse branches, we have the linear inductors L_1 and L_2, and the nonlinear resistances (NLR^1) and (NLR^2). The nonlinear resistances introduce nonlinear dispersion in the network, which is responsible for the compactification of pulse signal.

Boltzmann constant, I_0 the saturation current, and q the electron charge. However, let us mention that NLR were introduced in NLTLs for signal processing applications and particularly for image and wave amplification [29–32] and are usually made of operational amplifiers, transistors, or multipliers. From Kirchhoff's laws, the circuit equations for the network are given by

$$\frac{dQ_{n,m}}{dt} = (i_n - i_{n+1}) + (i_m - i_{m+1}),$$
$$V_{n-1,m} - V_{n,m} = L_1\frac{d\left(i_n^{L1}\right)}{dt}, \quad V_{n,m-1} - V_{n,m} = L_2\frac{d\left(i_m^{L2}\right)}{dt},$$
$$i_n = i_n^{L1} + i_n^{NLR1}, \quad n = 1,\ldots,N-1,$$
$$i_m = i_m^{L2} + i_m^{NLR2}, \quad m = 1,\ldots,M-1, \tag{3}$$

where i_n^{L1} and i_m^{L2} are the current passing through the self L_1 and L_2, respectively, while i_n^{NLR1} and i_m^{NLR2} are the current passing through the NLR in n and m directions, respectively. From Eqs. (1) and (2), the circuit equations (3) can be combined and rewritten into the following set of differential equations governing the propagation of the signal voltage in the network:

$$C_0V_0\frac{d^2}{dt^2}[\ln(1+V_{n,m}/V_0)] = \frac{1}{L_1}(V_{n+1,m}+V_{n-1,m}-2V_{n,m}) + \frac{1}{L_2}(V_{n,m+1}+V_{n,m-1}-2V_{n,m}) + I_{01}\frac{d}{dt}\left[\exp\left(\frac{V_{n-1,m}-V_{n,m}}{V_T}\right)\right.$$
$$\left. - \exp\left(\frac{V_{n,m}-V_{n+1,m}}{V_T}\right)\right] + I_{02}\frac{d}{dt}\left[\exp\left(\frac{V_{n,m-1}-V_{n,m}}{V_T}\right) - \exp\left(\frac{V_{n,m}-V_{n,m+1}}{V_T}\right)\right]. \tag{4}$$

Assuming that the signal voltage amplitude is sufficiently weak, Eq. (4) can be expanded as a power series of the local signal voltage $V_{n,m}$ to give the following set of differential equations governing small amplitude signal voltage in the network:

$$\frac{d^2V_{n,m}}{dt^2} + \left(u_{01}^2 + u_{01}g_{01}\frac{d}{dt}\right)(2V_{n,m}-V_{n+1,m}-V_{n-1,m}) + \left(u_{02}^2 + u_{02}g_{02}\frac{d}{dt}\right)(2V_{n,m}-V_{n,m+1}-V_{n,m-1})$$
$$= \alpha\frac{d^2V_{n,m}^2}{dt^2} + u_{01}\gamma_1\frac{d}{dt}[(V_{n-1,m}-V_{n,m})^2 - (V_{n,m}-V_{n+1,m})^2] + u_{02}\gamma_2\frac{d}{dt}[(V_{n,m-1}-V_{n,m})^2 - (V_{n,m}-V_{n,m+1})^2], \tag{5}$$

where $u_{01} = 1/\sqrt{L_1C_0}$ and $u_{02} = 1/\sqrt{L_2C_0}$ are characteristic frequencies of the network in n and m directions, respectively. The parameters are as follows: $\alpha = 1/(2V_0)$ is the measure of the standard nonlinearity, $\gamma_1 = I_{01}/(2C_0u_{01}V_T^2)$ and $\gamma_2 = I_{02}/(2C_0u_{02}V_T^2)$ are the measure of the diffusion nonlinearity, while terms proportional to $g_{01} = I_{01}/(C_0u_{01}V_T)$ and $g_{02} = I_{02}/(C_0u_{02}V_T)$ may be viewed as losses of the network, respectively, in n and m directions.

The linear properties of the network can be studied by assuming a dissipative sinusoidal wave in the form

$$V_{n,m}(t) = V_0\exp[-(\chi_1n+\chi_2m)] \times \exp[j(k_1n+k_2m-\omega t)] + \text{c.c.}, \tag{6}$$

where k_i and χ_i, $i = 1,2$ are the real and imaginary parts of the wave number $\tilde{k}$, ω is the angular frequency of the signal, and c.c. stands for the complex conjugation of the first term. Substituting Eq. (6) into Eq. (5) and equating real and imaginary parts, neglecting nonlinear terms leads to the following dispersion relation:

$$\omega = u_{01}g_{01}\sinh(\chi_1)\sin(k_1) + u_{02}g_{02}\sinh(\chi_2)\sin(k_2) + [(u_{01}g_{01}\sinh(\chi_1)\sin(k_1) + u_{02}g_{02}\sinh(\chi_2)\sin(k_2))^2 + 2u_{01}^2(1-\cosh(\chi_1)\cos(k_1)) + 2u_{02}^2(1-\cosh(\chi_2)\cos(k_2))]^{1/2}. \tag{7}$$

Similarly, χ_i, with $i = 1,2$ are expressed as follows:

$$\chi_i = \ln\left[\frac{\omega g_{0i} + \sin(k_i)\sqrt{u_{0i}^2 + \omega^2g_{0i}^2}}{u_{0i}\sin(k_i) + \omega g_{0i}\cos(k_i)}\right], \quad i = 1,2. \tag{8}$$

It is easy to show that, when $g_{01} = g_{02} = 0$, that is in the absence of losses, Eq. (8) reduces to the following dispersion relation of the nondissipative two-dimensional NLTL

$$\omega = 2\left[u_{01}^2\sin^2(k_1/2) + u_{02}^2\sin^2(k_2/2)\right]^{1/2}. \tag{9}$$

This relation justifies the low pass filter character of the network with the cutoff frequency $\omega_c = 2\sqrt{u_{01}^2 + u_{02}^2}$. The expression (8) for the rate of dissipation of the signal amplitude in the network indicates that the amplitude of the signal decreases in the n and m directions as a function of the wave number in both directions.

III. TWO-DIMENSIONAL NONLINEAR DIFFUSIVE BURGERS EQUATION AND SOME PROPERTIES

Equation (5) is the set of $N \times M$ differential equations which in general are very difficult to solve, and their solutions need to be approximated via the integrable equations easy to solve. Assuming that the wavelength is sufficiently large as compared to the length of one section, we can use the continuum medium approximations by introducing the continuous space variables $x = nh$ and $y = mh$, and replacing the differences by differentials. Hence the signal voltage at

(n,m)th node, $V_{n,m}(t)$, is replaced by the function of real variables x, y, and t, that is $V(x,y,t)$, where h is the lattice spacing. Accordingly, Eq. (5) leads to the following two-dimensional partial differential equation:

$$\frac{\partial^2 V}{\partial t^2} - u_{01}^2\frac{\partial^2 V}{\partial x^2} - u_{02}^2\frac{\partial^2 V}{\partial y^2} - \alpha\frac{\partial^2 (V^2)}{\partial t^2} + u_{01}\gamma_1\frac{\partial^2}{\partial t\partial x}\left[\left(\frac{\partial V}{\partial x}\right)^2\right] + u_{02}\gamma_2\frac{\partial^2}{\partial t\partial y}\left[\left(\frac{\partial V}{\partial y}\right)^2\right] = u_{01}g_{01}\frac{\partial^3 V}{\partial t\partial x^2} + u_{02}g_{02}\frac{\partial^3 V}{\partial t\partial y^2}, \tag{10}$$

where, without loss of generality, the lattice spacing h is taken equal to one so that the space variables x and y are given in unit of cell, since in NLTL the width of unit cell is less relevant because it does not characterize the spatial extension of the cell as it is the case for other systems, such as in solid-state physics [26]. We first introduce a small parameter $\epsilon \ll 1$ and the following change of variables:

$$V = \epsilon\phi(X,Y,\tau), \quad X = \epsilon^0(x - v_{p1}t), \quad Y = \epsilon^0(y - v_{p2}t), \quad \tau = \epsilon^1 t, \tag{11}$$

in order to eliminate linear dispersion and guarantee the balance between higher and diffusive nonlinearities. Next, substituting the set of Eqs. (10) into Eq. (11), assuming $g_{01} = \epsilon^2\lambda_1$ and $g_{02} = \epsilon^2\lambda_2$ (which means that the dissipation effect of the network is weak), and assembling the resulting equationlike powers of ϵ, we obtain a sequence of nonlinear equations. At the lowest order, that is at order ϵ, one has

$$\left(v_{p1}^2 - u_{01}^2\right)\frac{\partial^2\phi}{\partial X^2} + \left(v_{p2}^2 - u_{02}^2\right)\frac{\partial^2\phi}{\partial Y^2} + 2v_{p1}v_{p2}\frac{\partial^2\phi}{\partial X\partial Y} = 0. \tag{12}$$

Next, considering terms of order ϵ^2, it follows that

$$\hat{L}\left(2\frac{\partial\phi}{\partial\tau} + \alpha v_{p1}\frac{\partial}{\partial X}(\phi^2) + \alpha v_{p2}\frac{\partial}{\partial Y}(\phi^2) + 2u_{01}\gamma_1\frac{\partial\phi}{\partial X}\frac{\partial^2\phi}{\partial X^2} + 2u_{02}\gamma_2\frac{\partial\phi}{\partial Y}\frac{\partial^2\phi}{\partial Y^2} - \epsilon u_{01}\lambda_1\frac{\partial^2\phi}{\partial X^2} - \epsilon u_{02}\lambda_2\frac{\partial^2\phi}{\partial Y^2}\right) = 0, \tag{13}$$

where the operator $\hat{L} = v_{p1}\frac{\partial}{\partial X} + v_{p2}\frac{\partial}{\partial Y}$ is the linear combination of differentiations $\frac{\partial}{\partial X}$ and $\frac{\partial}{\partial Y}$. Integrating once this equation and setting the constant of integration to zero, yields the following perturbed two-dimensional NLDB equation:

$$\frac{\partial\phi}{\partial\tau} + \frac{\alpha v_{p1}}{2}\frac{\partial(\phi^2)}{\partial X} + \frac{\alpha v_{p2}}{2}\frac{\partial(\phi^2)}{\partial Y} + u_{01}\gamma_1\frac{\partial\phi}{\partial X}\frac{\partial^2\phi}{\partial X^2} + u_{02}\gamma_2\frac{\partial\phi}{\partial Y}\frac{\partial^2\phi}{\partial Y^2} = \epsilon\left(\frac{u_{01}\lambda_1}{2}\frac{\partial^2\phi}{\partial X^2} + \frac{u_{02}\lambda_2}{2}\frac{\partial^2\phi}{\partial Y^2}\right), \tag{14}$$

where the dissipation is introduced by terms proportional to ϵ. Let us notice that in the absence of the dissipative terms (that is when $\lambda_1 = \lambda_2 = 0$), the above equation reduces to

$$\frac{\partial\phi}{\partial\tau} + \frac{\alpha v_{p1}}{2}\frac{\partial(\phi^2)}{\partial X} + \frac{\alpha v_{p2}}{2}\frac{\partial(\phi^2)}{\partial Y} + u_{01}\gamma_1\frac{\partial\phi}{\partial X}\frac{\partial^2\phi}{\partial X^2} + u_{02}\gamma_2\frac{\partial\phi}{\partial Y}\frac{\partial^2\phi}{\partial Y^2} = 0. \tag{15}$$

As the one-dimensional nonlinear extended KdV equation introduced by Rosenau and co-workers [4], this equation is invariant under the transformation $\phi \to \nu\phi$, $\tau \to \tau/\nu$, ν being an arbitrary constant, which had been proved to be the necessary condition to have compact solutions whose width is independent of the amplitude. Similarly, this equation possesses the mass as a conserved quantity (see the Appendix)

$$I_1 = \int \phi\, d\eta, \tag{16}$$

where η is the linear combination of space variables X and Y (that is $\eta = aX + bY$), meaning that in any arbitrary propagation direction, there is a detailed balance between nonlinear convection (terms proportional to α) and nonlinear diffusion. When $v_{p2} = \gamma_2 = 0$, this equation reduces to the well-known one-dimensional NLDB equation obtained in [27] admitting the pulse solitary wave with compact support as a solution. Equation (15) appears then as the two-dimensional generalization of this preceding one-dimensional case.

IV. SOLUTIONS OF THE TWO-DIMENSIONAL NLDB EQUATION

The focal point here corresponds to the determination of the solutions of Eqs. (14) and (15). Before the discovery of solitons, mathematicians thought that nonlinear differential equations could not be solved, at least not exactly. With the development of soliton theory, many powerful methods for obtaining the exact solutions of soliton equations have been presented [33–38]. In the present paper, and in order to derive the quantitative effects of the dissipation terms, we use an approach based on the multiple time scale expansion [27,39] which has been proved to be convenient for studying the time-dependent perturbations on standard soliton motion and nonlinear evolution equations admitting solitons with compact shape as solution.

A. Undamped two-dimensional NLDB equation

Let us first start from the two-dimensional NLDB equation (15), which is just Eq. (14) with $\epsilon = 0$. To find the traveling-waves solutions of this equation, we define the single variable

$$\eta = X\cos(\theta) + Y\sin(\theta) - v_c\tau, \tag{17}$$

where v_c is the front wave velocity and θ the propagation direction of the wave. By taking into account this definition into Eq. (12), the following ordinary differential equation is obtained:

$$\left[\left(v_{p1}^2 - u_{01}^2\right)\cos^2(\theta) + \left(v_{p2}^2 - u_{02}^2\right)\sin^2(\theta) + 2v_{p1}v_{p2}\sin(\theta)\cos(\theta)\right]\phi'' = 0, \tag{18}$$

where the prime stands for derivative with respect to η. The above equation is unconditionally true if its coefficient is equal to zero, leading to

$$v_{p1} = u_0 \cos(\theta), \quad v_{p2} = u_0 \sin(\theta),$$
$$u_0 = \sqrt{u_{01}^2 \cos^2(\theta) + u_{02}^2 \sin^2(\theta)}. \tag{19}$$

By substituting (18) and (19) into Eq. (15), the following nonlinear ordinary differential equation is obtained:

$$\{-v_c + \alpha u_0 \phi + [u_{01}\gamma_1 \cos^3(\theta) + u_{02}\gamma_2 \sin^3(\theta)]\phi''\}\phi' = 0. \tag{20}$$

From the above equation, the following first integral is obtained:

$$\phi'^2 + \tilde{\mu}\left(\phi - \frac{v_c}{\alpha u_0}\right)^2 = c_1, \tag{21}$$

with $\tilde{\mu} = \alpha u_0/[u_{01}\gamma_1 \cos^3(\theta) + u_{02}\gamma_2 \sin^3(\theta)]$, where c_1 is the constant of integration. It is important to mention that Eq. (20) can be derived from the auxiliary Hamiltonian H_a or the Lagrangian L_a defined as follows:

$$H_a = \tfrac{1}{2}m(\phi)[\phi'^2 + W(\phi)],$$
$$L_a = \tfrac{1}{2}m(\phi)[\phi'^2 - W(\phi)]. \tag{22}$$

This Hamiltonian is viewed as the energy of a particle of effective mass $m(\phi) = 1$ moving in the effective potential

$$W(\phi) = \tilde{\mu}\left(\phi - \frac{v_c}{\alpha u_0}\right)^2, \tag{23}$$

where ϕ would represent the position and η the time. The behavior of the system may be easily studied by means of the phase plane plot which is the best way for observing the evolution of the variable ϕ. It is obvious that Eq. (20) can be transformed into the following autonomous dynamic system:

$$\phi' = 0, \quad \text{or} \quad \begin{cases} \frac{d\phi}{d\eta} = \phi', \\ \frac{d\phi'}{d\eta} = \tilde{\mu}\left(\frac{v_c}{\alpha u_0} - \phi\right), \end{cases} \tag{24}$$

admitting ($\phi' = 0$, $\phi = v_c/\alpha u_0$) as a solution, which is the equilibrium point of the system. From the linear stability analysis [40], it appears that this equilibrium point is a saddle point if $\tilde{\mu} < 0$ [provided that $d^2(W(\phi))/d\phi^2 < 0$ at $\phi = v_c/\alpha u_0$], and a center point elsewhere. As $\phi' = 0$ is a solution of Eq. (20), any arbitrary constant is the solution of Eq. (15), meaning that the solution of Eq. (15) can be localized in a finite region of space and would be a constant (including zero) outside this region.

When $\tilde{\mu} < 0$, the phase-space plot (not sketched here) shows trajectories passing through the origin corresponding to solution decaying exponentially, which is the solution verifying the nonvanishing boundary conditions, and subjected to the constraints

$$\lim_{\eta\to\pm\infty} \phi = A_0, \quad \lim_{\eta\to\pm\infty} \frac{\partial^n \phi}{\partial \eta^n}, \quad n = 1,2,\ldots = 0. \tag{25}$$

With the above constraints, and from Eq. (21) it follows that the constant of integration $c_1 = 0$ and the velocity of the wave satisfies the relation

$$v_c = \alpha u_0 A_0 \tag{26}$$

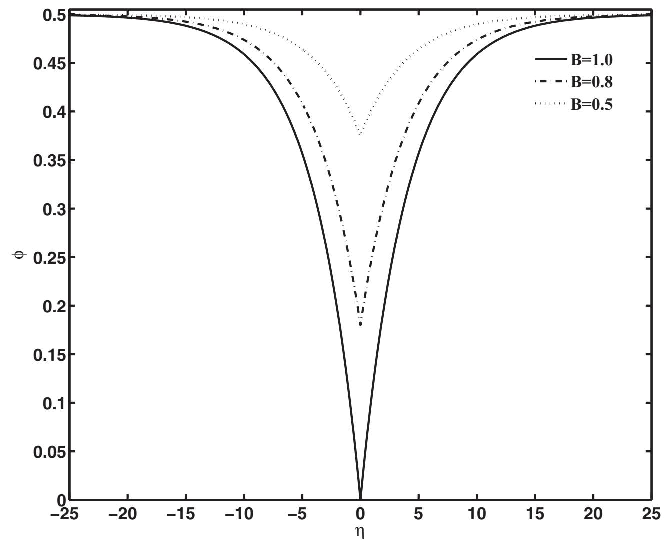

FIG. 2. Cusp solitary wave profile according to Eq. (27), with parameters $A_0 = 0.5$, $\mu_c = 0.25$ and for different values of the depth parameter B: 0.5, 0.8, and 1.

within these conditions; Eq. (21) admits the following solution

$$\phi(\eta) = A_0[1 - B^2 \exp(-\mu_p|\eta - \eta_0|)], \tag{27}$$

where B is a free parameter and $\mu_p = \sqrt{-\tilde{\mu}}$, provided that $\tilde{\mu}$ is negative, that is $\alpha[u_{01}\gamma_1 \cos^3(\theta) + u_{02}\gamma_2 \sin^3(\theta)] < 0$, which is the necessary condition for the system to exhibit this solution. As presented in Fig. 2, the signal profile associated with this solution exhibits a dip corresponding to the cusp solitary wave. Parameters A_0 and η_0 represent the amplitude and the dip localization, respectively, while B designates the depth parameter.

For $\tilde{\mu} > 0$, the phase-space plot (not sketched here) exhibits closed trajectories centered at the equilibrium point, which evidences [associated to the fact that any arbitrary constant is the solution of Eq. (16)] the existence of solution strictly localized in a finite region of space and zero outside this region, the compactlike pulse signal. This particular solution verifies the following vanishing boundary conditions, and the conditions at the maximum amplitude

$$\lim_{|\eta|\to\infty} \frac{d^k\phi}{d\eta^k} = 0, \quad \text{with } k = 0,1,2,3,\ldots. \tag{28}$$

In addition, the maximum amplitude has to satisfy the relation

$$\lim_{\eta\to\eta_0} \phi = A_0, \quad \lim_{\eta\to\eta_0} \frac{d\phi}{d\eta} = 0. \tag{29}$$

Accordingly, $c_1 = \tilde{\mu} v_c^2/(\alpha^2 u_0^2)$ and $v_c = \alpha u_0 A_0/2$, leading to the following equation: $\phi'^2 = \tilde{\mu}\phi(A_0 - \phi)$. This equation can be integrated exactly to give the following solitary wave with compact support:

$$\phi(\eta) = \begin{cases} A_0 \cos^2(\mu_c \eta), & |\eta| \leqslant \pi/(2\mu_c), \\ 0, & |\eta| > \pi/(2\mu_c), \end{cases} \tag{30}$$

with width parameter $\mu_c = (\sqrt{\tilde{\mu}})/2$, provided that the following constraint is satisfied: $\alpha[u_{01}\gamma_1 \cos^3(\theta) + u_{02}\gamma_2 \sin^3(\theta)] > 0$. The conserved quantity associated to this solution can be easily calculated from Eq. (16) and read

$$I_1 = \frac{\pi A_0}{2\mu_c}. \quad (31)$$

In Fig. 2, the compacton width $L_p = \pi/\mu_c$ is plotted as a function of the reduced propagation direction θ/π, for $\alpha = 0.25$, $\gamma_1 = 0.65476$, and for different choice of other parameters. This result indicates that in contrast to a one-dimensional compact pulse where the width is constant and solely set by the parameters of the waveguide, the compacton widths obtained here are a function of the propagation direction. In what follows, we will focus our attention in the case $\tilde{\mu} > 0$ only, which as shown in Fig. 2 as the only case adequate to the network under consideration.

B. Damped two-dimensional NLDB equation

In order to find the solution of Eq. (14) and then analyze the dissipative effect of the network, it is important to mention that many wave equations consist in generalizations of the integrable equations like the KdV equation and, sometimes, additional terms may be considered as small perturbations. The basic idea of the perturbation approach is to look for a solution of a perturbed nonlinear equation in terms of certain natural fast and slow variables. We assume that a solution ϕ is of the form

$$\phi = \phi_0 + \epsilon\phi_1 + \cdots, \quad (32)$$

where $\phi_1, \ldots$ are corrections, while the independent variables are transformed into several variables $\tau_j = \epsilon^j \tau$, $j = 0,1,2,\ldots$ and where ϕ_j satisfy the vanishing boundary conditions (28).

Substituting the above expression of ϕ into Eq. (14) and collecting the powers of ϵ we obtain the series of equations which lead at the lowest order ϵ^0 to Eq. (15) with $\phi \equiv \phi_0$, where the solution given by Eq. (30) can be rewritten as

$$\phi_0(\tilde{\eta}) = \begin{cases} \tilde{A}_0(\tau_1,\ldots)\cos^2(\mu_c\tilde{\eta}), & |\tilde{\eta}| \leqslant \pi/(2\mu_c), \\ 0, & |\tilde{\eta}| > \pi/(2\mu_c), \end{cases} \quad (33)$$

with

$$\frac{\partial\tilde{\eta}}{\partial\tau_0} = -v_c(\tau_1,\ldots) = -\frac{\alpha u_0\tilde{A}_0(\tau_1,\ldots)}{2},$$
$$\frac{\partial\tilde{\eta}}{\partial X} = \cos(\theta), \quad \frac{\partial\tilde{\eta}}{\partial Y} = \sin(\theta). \quad (34)$$

The first-order term in ϵ obeys the following inhomogeneous linear differential equation in ϕ_1:

$$\hat{L}_r(\phi_1) = \frac{u_{01}\lambda_1}{2}\frac{\partial^2\phi_0}{\partial X^2} + \frac{u_{02}\lambda_2}{2}\frac{\partial^2\phi_0}{\partial Y^2} - \frac{\partial\phi_0}{\partial\tau_1}, \quad (35)$$

where $\hat{L}_r$ is the linear operator defined by

$$\hat{L}_r = \frac{\partial}{\partial\tau_0} + \alpha v_{p1}\left(\phi_0\frac{\partial}{\partial X} + \frac{\partial\phi_0}{\partial X}\right) + \alpha v_{p2}\left(\phi_0\frac{\partial}{\partial Y} + \frac{\partial\phi_0}{\partial Y}\right)$$
$$+ u_{01}\gamma_1\left(\frac{\partial\phi_0}{\partial X}\frac{\partial^2}{\partial X^2} + \frac{\partial^2\phi_0}{\partial X^2}\frac{\partial}{\partial X}\right)$$
$$+ u_{02}\gamma_2\left(\frac{\partial\phi_0}{\partial Y}\frac{\partial^2}{\partial Y^2} + \frac{\partial^2\phi_0}{\partial Y^2}\frac{\partial}{\partial Y}\right). \quad (36)$$

Denoting by ρ_i ($i = 1,\ldots,M$) the ith solution of the homogeneous adjoint problem $\hat{L}_r^A(\rho_i) = 0$, where $\hat{L}_r^A$ defined by

$$\hat{L}_r^A = \frac{\partial}{\partial\tau_0} + \alpha v_{p1}\phi_0\frac{\partial}{\partial X} + \alpha v_{p2}\phi_0\frac{\partial}{\partial Y} + u_{01}\gamma_1\frac{\partial\phi_0}{\partial X}\frac{\partial^2}{\partial X^2}$$
$$+ u_{02}\gamma_2\frac{\partial\phi_0}{\partial Y}\frac{\partial^2}{\partial Y^2} \quad (37)$$

is the adjoint operator to $\hat{L}_r$, we obtain by multiplying Eq. (35) by ρ_i the following differential equation:

$$\hat{L}_r(\phi_1)\rho_i - \hat{L}_r^A(\rho_i)\phi_1$$
$$= \left(\frac{u_{01}\lambda_1}{2}\frac{\partial^2\phi_0}{\partial X^2} + \frac{u_{02}\lambda_2}{2}\frac{\partial^2\phi_0}{\partial Y^2} - \frac{\partial\phi_0}{\partial\tau_1}\right)\rho_i. \quad (38)$$

Using the boundary conditions (28) at infinity, this equation may be integrated to give the following secularity condition for Eq. (35):

$$\int_{-\pi/(2\mu_c)}^{\pi/(2\mu_c)} \rho_i\left(\frac{\lambda}{2}\frac{\partial^2\phi_0}{\partial\tilde{\eta}^2} - \frac{\partial\phi_0}{\partial\tau_1}\right)d\eta = 0, \quad (39)$$

with $\lambda = u_{01}\lambda_1\cos^2(\theta) + u_{02}\lambda_2\sin^2(\theta)$. Then the secularity condition (39) with $\rho_1 = \phi_0$ leads to the following differential equation $\partial\tilde{A}_0/\partial\tau_1 + 2\lambda\mu_c^2\tilde{A}_0/3 = 0$, which may be integrated to give the following dependency of amplitude $\tilde{A}_0$ on time τ_1:

$$\tilde{A}_0(\tau_1) = A_0\exp\left[-\tfrac{2}{3}\lambda\mu_c^2\tau_1\right], \quad (40)$$

which vanishes for increasing values of τ_1. The function ϕ_1 is a solution of the linear inhomogeneous ordinary differential equation (35) which, according to the transformation (17), yields the following differential equation:

$$\frac{\partial^2\phi_1}{\partial\eta^2} + 4\mu_c^2\phi_1 = \frac{4\mu_c^2}{\alpha u_0(\partial\phi_0/\partial\eta)}\left(\frac{\lambda}{2}\frac{\partial^2\phi_0}{\partial\eta^2} - \frac{\partial\phi_0}{\partial\tau_1}\right). \quad (41)$$

By substituting (33) into the above equation and solving the resulting equation, we get

$$\phi_1(\tilde{\eta}) = \frac{\lambda\mu_c}{3\alpha u_0}\bigg[(2\mu_c|\tilde{\eta}| - \pi)\cos(2\mu_c\tilde{\eta})$$
$$+ \sin(2\mu_c\tilde{\eta})\log\left(\frac{|\tan(\mu_c\tilde{\eta})|}{2\cos^2(\mu_c\tilde{\eta})}\right)\bigg], \quad (42)$$
$$|\tilde{\eta}| \leqslant \pi/(2\mu_c).$$

As one can see, ϕ_1 is not a decreasing function of time, predicting then the widening of the pulse widths when the initial signal amplitude decreases. By using original variables, the dissipative compactlike pulse solitary wave solution of the two-dimensional NLDB equation (14) is given by

$$\phi(X,Y,\tau) = A_0\exp\left(-\frac{2}{3}\epsilon\lambda\mu_c^2\tau\right)\cos^2(\mu_c\eta)$$
$$+ \frac{\epsilon\lambda\mu_c}{3\alpha u_0}\bigg[(2\mu_c|\eta| - \pi)\cos(2\mu_c\eta)$$
$$+ \sin(2\mu_c\eta)\log\left(\frac{|\tan(\mu_c\eta)|}{2\cos^2(\mu_c\eta)}\right)\bigg],$$
$$|\eta| \leqslant \pi/(2\mu_c), \quad (43)$$

while $\eta \equiv \eta(X,Y,\tau)$ is obtained by solving Eq. (33), remembering that $\tau_0 = \tau$ and $\tau_1 = \epsilon\tau$, leading to

$$\eta(X,Y,\tau) = X\,\cos(\theta) + Y\,\sin(\theta) - \frac{3\alpha u_0 A_0}{4\epsilon\lambda\mu_c^2}\left[1 - \exp\left(-\frac{2}{3}\lambda\mu_c^2\epsilon\tau\right)\right]. \tag{44}$$

Finally, we find the following two-dimensional dissipative compactlike signal voltage for the network:

$$V_{n,m}(t) = V_0\exp\left[-\frac{2}{3}\left(u_{01}g_{01}\cos^2(\theta) + u_{02}g_{02}\sin^2(\theta)\right)\mu_c^2 t\right]\cos^2(\mu_c\eta_{n,m}(t)) + \frac{\mu_c}{3\alpha u_0}[u_{01}g_{01}\cos^2(\theta) + u_{02}g_{02}\sin^2(\theta)]$$
$$\times\left\{(2\mu_c|\eta_{n,m}(t)| - \pi)\cos(2\mu_c\eta_{n,m}(t)) + \sin(2\mu_c\eta_{n,m}(t))\log\left(\frac{|\tan(\mu_c\eta_{n,m}(t))|}{2\,\cos^2(\mu_c\eta_{n,m}(t))}\right)\right\}, \quad |\eta_{n,m}(t)| \leqslant \pi/(2\mu_c), \tag{45}$$

where $\eta_{n,m}(t)$ is given by

$$\eta_{n,m}(t) = n\,\cos(\theta) + m\,\sin(\theta) - u_0 t - \frac{3\alpha u_0 V_0}{4(u_{01}g_{01}\cos^2(\theta) + u_{02}g_{02}\sin^2(\theta))\mu_c^2}$$
$$\times\left[1 - \exp\left(-\frac{2}{3}(u_{01}g_{01}\cos^2(\theta) + u_{02}g_{02}\sin^2(\theta))\mu_c^2 t\right)\right], \tag{46}$$

while the signal velocity is obtained from $v_s = -d(\eta_{n,m}(t))/dt$, leading to

$$v_s = u_0\left[1 + \frac{\alpha V_0}{2}\exp\left(-\frac{2}{3}(u_{01}g_{01}\cos^2(\theta) + u_{02}g_{02}\sin^2(\theta))\mu_c^2 t\right)\right]. \tag{47}$$

It is obvious from this expression that there may be decay of the initial velocity and the amplitude of the compactlike pulse solitary wave (45), which is qualitatively in agreement with the results previously obtained in some one-dimensional model by Rosenau and Pikovsky [8] and recently by Rus and Villatoro [41] by means of conserved quantities of the $K(2,2)$ equation. When $g_{01} = g_{02} = 0$, Eqs. (45) and (46) lead to the following compactlike pulse signal:

$$V_{n,m}(t) = \begin{cases} V_0\cos^2\left[\mu_c\left(n\,\cos(\theta) + m\,\sin(\theta) - tu_0\left(1 + \frac{\alpha V_0}{2}\right)\right)\right], \\ \qquad |n\,\cos(\theta) + m\,\sin(\theta) - tu_0(1 + \alpha V_0/2)| \leqslant \pi/(2\mu_c), \\ 0, \qquad |n\,\cos(\theta) + m\,\sin(\theta) - tu_0(1 + \alpha V_0/2)| > \pi/(2\mu_c) \end{cases} \tag{48}$$

for the nondissipative two-dimensional electrical network, and the envelope velocity (47) reduces to $v_s = u_0(1 + \alpha V_0/2)$, which is linearly dependent of the amplitude V_0 of the signal.

V. NUMERICAL EXPERIMENTS

A. Numerical details

In this section, we present the details and the results of numerical integrations performed both on the realistic discrete equations governing wave propagation along the network (5) as well as on the two-dimensional NLDB-type equation (15) describing the propagation of small-amplitude signal voltages in the network. Our first goal is to validate our continuum model by comparing their predictions against numerical solutions of the underlying semidiscrete equations. Our second goal is to demonstrate that the two-dimensional compact pulse obtained in this work has properties similar to those previously found by Rosenau and Hyman on their generalized KdV equation. To this end, let us consider the network as described in Sec. II, with the following numerical values: $L_1 = L_2 = 0.47$ mH for the inductors in the n and m directions. The nonlinear capacitor in the shunt branch is the varactor diode with the characteristic parameters $C_0 = 320$ pF and $\alpha = 0.25V^{-1}$, at the operating point $V_0 = 2V$. The nonlinear resistors in the series branches are identical in both n and m directions and are the standard diodes with the saturation current $I_{01} = I_{02} = 6.75346 \times 10^{-7}A$, leading for $V_T = 25$ mV to the characteristic parameters $\gamma_1 = \gamma_2 = 0.65476$ cell$^{-1}V^{-1}$ and $g_{01} = g_{02} = 3.2738 \times 10^{-2}$ cell^{-1}. With these numerical values of the network elements, the characteristic parameters can then be computed as $u_{01} = u_{02} = 2.5786 \times 10^6$ cell/s, which allows us to compute the compactlike pulse width $L_p = \pi/\mu_p$, plotted in Fig. 3 (solid line) as a function of the reduced propagation direction θ/π. It is obvious that $L_p \gg 1$, that is 11.5296 cells $\leqslant L_p \leqslant$ 13.7110 cells, and consequently the use of the continuum limit approximations may be justified.

B. Simulation results

1. *Two-dimensional nonlinear diffusive Burgers equation: Two-dimensional transverse pulse compactons*

In order to verify the analytical predictions, we perform here numerical integrations of the two-dimensional NLDB-type equation (15), which is an approximation of the exact equation governing signal propagation in the network. The fourth-order Adams-Bashforth-Moulton predictor corrector method in time and the finite difference method in space with nonreflecting boundary conditions are used with normalized integration step $\Delta\tau = 0.0011$. Similarly, we have used $N = M = 1024$ spatial grid points and the finite difference method is implemented in the computer by means of the gradient function of the MATLAB toolbox. In order to rewrite Eq. (15) in a nondimensional form more appropriate for numerical simulations, we have defined the following dimensionless quantities $T = \alpha u_0\mu_c\tau$, $X' = 2\mu_c X$, and $Y' = 2\mu_c Y$.

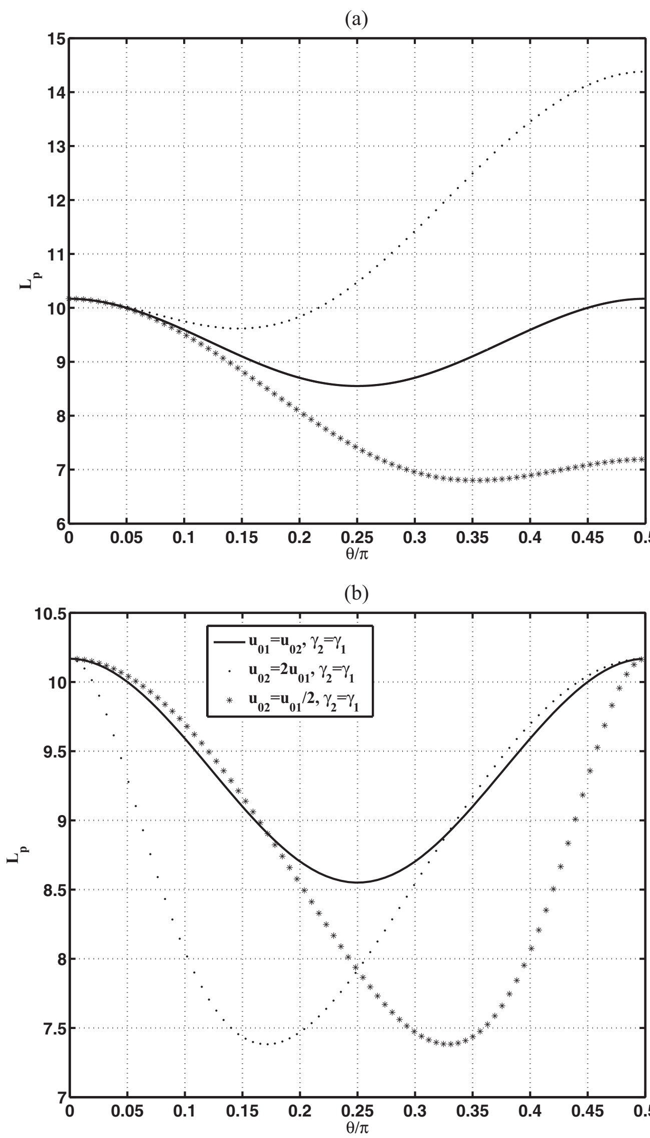

FIG. 3. Pulse widths L_p as a function of the propagation direction θ and for parameters $\alpha = 0.25V^{-1}$, $\gamma_1 = 0.65476$ cell$^{-1}V^{-1}$, and for different values of u_{01}, u_{02}, and γ_2.

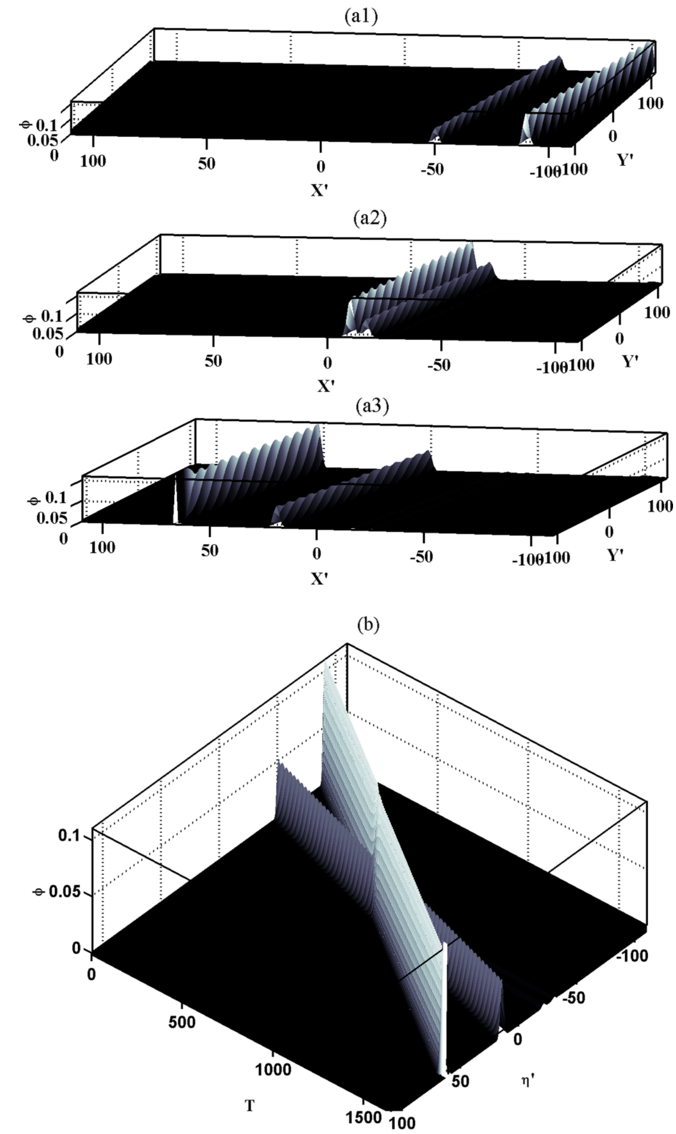

FIG. 4. (Color online) Propagation and elastic collision of two compactons described by Eq. (50) for $\theta = \pi/64$, with amplitudes 0.11 and 0.5. As one can see these compactons remained coherent after collision.

Accordingly, for $u_{01} = u_{02}, \gamma_1 = \gamma_2$, and $\epsilon = 0$, one obtains

$$\frac{\partial\phi}{\partial T} + \cos(\theta)\frac{\partial(\phi^2)}{\partial X'} + \sin(\theta)\frac{\partial(\phi^2)}{\partial Y'} + \frac{1}{\cos^3(\theta)+\sin^3(\theta)} \times\left[\frac{\partial}{\partial X'}\left(\left(\frac{\partial\phi}{\partial X'}\right)^2\right) + \frac{\partial}{\partial Y'}\left(\left(\frac{\partial\phi}{\partial Y'}\right)^2\right)\right] = 0. \quad (49)$$

As initial condition, we have considered the following pulse compacton:

$$\phi(\eta) = \begin{cases} A_0\cos^2(\eta'/2), & |\eta'| \leqslant \pi, \\ 0, & |\eta'| > \pi, \end{cases} \quad (50)$$

with $\eta' = (X' - X_0')\cos(\theta) + (Y' - Y_0')\sin(\theta) - A_0 T$, which is the exact solution of Eq. (49). With this dimensionless form, the conserved quantity is given by $I_1 = \pi A_0$. Figure 4 illustrates the elastic collision of two pulselike compact solitary waves, with different amplitudes $A_{01} = 0.11$ and $A_{02} = 0.051$ and with the propagation direction $\theta = \pi/64$, (a) is the representation in (X',Y') plane, while (b) is the projection in the (η',T) plane. Since the taller one moves faster than the shorter one, it catches up and collides with the shorter one and then moves away from it as time increases. It is obvious that these compact solitary waves on collision reemerge as compactons, with a tiny amount of energy going into a zero mass ripple which eventually reemerges into compacton-anticompacton pair of small (<5%) amplitude, which is in full agreement with results found in numerical experiments by Rosenau and Hyman [4] and recently by Ndjanfang and co-workers [27]. Figure 5 illustrates the elastic collision of above two-dimensional compactlike pulse solitary waves and an anticompacton [in the (η',T) plane] propagating in opposite directions. We note the production of the "pair" of compacton anticompacton (with small amplitude $\sim 10^{-3}A_0$).

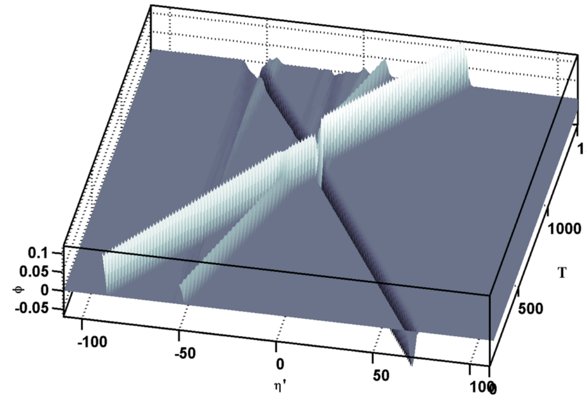

FIG. 5. (Color online) Propagation and elastic collision of two compactons and the anticompacton for $\theta = \pi/64$. The compactons with amplitudes 0.11 and 0.5 propagate in the forward direction, while the anticompacton with amplitude 0.07 propagate in the backward direction. As one can see they remain coherent after collision, but we note the "pair" production of small compacton and anticompacton (with amplitude $\sim 10^{-3} A_0$).

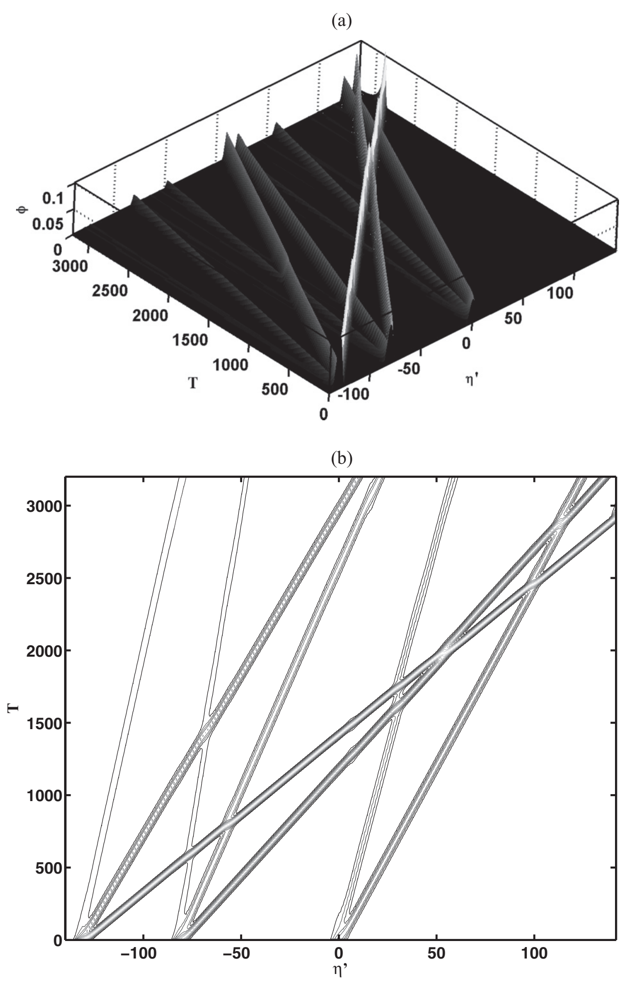

FIG. 6. (a) Pulses with initial widths two times that of the compacton of Eq. (50). It is obvious that the initial wide pulse breaks into compactons that collide elastically. (b) Contour plot of the evolution of the compactons.

Now, taking as initial conditions the compact wave packets with a width two times larger than that of the exact compact pulse solitary wave described by Eq. (50), as presented in Fig. 6, the signal decomposes into many compact pulses which collide elastically.

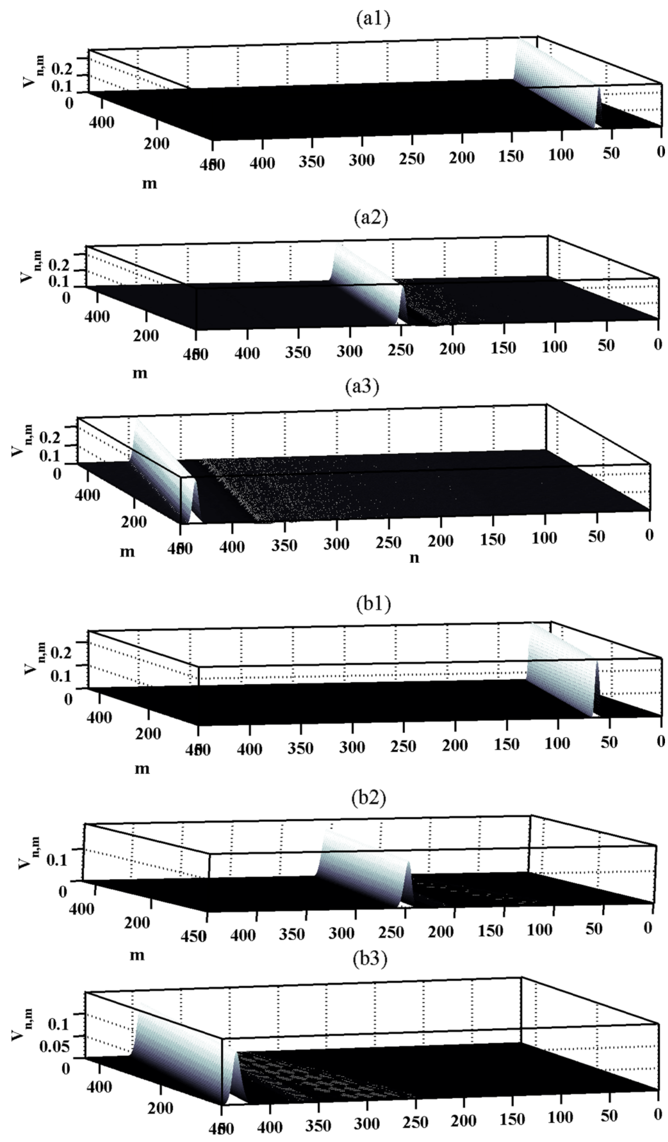

FIG. 7. (Color online) Compact signal voltage (in volts) as a function of the propagating direction n and transverse direction m of the network at given times of the propagation of wave: the initial signal voltage (1) is the compactlike pulse solitary wave located at cell $(n0,m0) = (60,60)$ with the initial amplitude $V_0 = 0.25V$, the propagation direction $\theta = \pi/64$, and the width $L_p = 10$ cells; (2) and (3) show the signal at given times of propagation (in units of $u_0 = \sqrt{u_{01}^2 \cos^2(\theta) + u_{02}^2 \sin^2(\theta)} = 2.5821 \times 10^6$): 96.3 and 192.6, respectively. (a) is the simulation of Eq. (5) without dissipation (that is for $g_{01} = g_{02} = 0$) and we note that the wave experiences a uniform and stable propagation along the network with the speed $v_s/u_0 = 1.02$, which is in good agreement with the analytically predicted value. (b) is the simulation of the exact Eq. (4) of the network. As one can see, the signal amplitude decreases in propagation due to the dissipation which cannot be neglected.

2. Two-dimensional transverse electrical pulse compacton

Next, we have integrated numerically the exact discrete equations (4) and (5) of the network, using the fourth-order Runge Kutta method with normalized integration time step $h = \left(u_{01}^2\cos^2(\theta) + u_{02}^2\sin^2(\theta)\right)^{1/2}\Delta t = 0.002$ corresponding to the sampling period $Ts = 0.77654$ ns, with the initial condition (48) and with the initial amplitude $V_0 = 0.25V$. Similarly, the number of cells is taken equal to $N = M = 450$ in the propagation and transverse directions. The corresponding initial compact solitary wave parameters are $\theta = \pi/64$ for the propagation direction, $\mu_c = 0.3097$ leading to $L_p = 10.143$ cells for the width, and $v_p/u_0 = (1 + \alpha V_0/2) = 1.02625$ for the reduced speed according to the analytical predictions.

In Fig. 7(a), we have shown the result obtained from Eq. (5) in the absence of dissipative terms from where we notice that the initial electrical signal voltage propagates with constant amplitude, without distortion of shape, and with constant reduced velocity 1.02, which is in agreement with the analytical predicted value.

In Fig. 7(b), the results of the direct integration of the exact Eq. (4) of the network is presented. It is obvious that the stable motion of the initial compact signal is observed, but with the decrease of its amplitude due to dissipation which cannot be neglected. It appears also that the compact pulse signal voltage widens as the amplitude decreases, which is understandable and is justified by the fact that (48) is not the exact solution of Eq. (4) and it eventually evolves into its exact solution given by (45) containing correction terms, through the network.

VI. CONCLUDING REMARKS

In this paper, the propagation of electrical compactlike pulse solitary wave in a two-dimensional nonlinear network was investigated both analytically and numerically. The compactification process results from the introduction of diodes, acting as nonlinear resistances in the series branches of the network in the propagation and transverse directions, respectively. Using the continuum limit approximations, we have shown that the dynamics of small amplitude signals in the network can be described by a two-dimensional nonlinear dissipative and diffusive Burgers equation. In the absence of the dissipative terms, this equation admits only the mass as the conserved quantity and can admit two types of solitary waves: the cusp solitary wave and the pulse compacton according to the magnitude of its coefficients. The exact analytical expression of these solutions are found and they bear interesting properties usually encountered in systems with nonlinear dispersion. We found that although the width of these signals only is independent of their amplitude, as is the case for KdV pulse compactons, the widths obtained here are functions of the direction of propagation of the signal voltage.

Next, using the perturbation method, the dissipation effects of the network were studied and it was found that signal voltage amplitude can decrease in propagation, but does not vanish completely due to the nondependency of the correction term on the input amplitude. Numerical integrations of the two-dimensional NLDB equation as well as the exact equations of the network have confirmed the analytical results.

Finally, it is important to mention that, since we have focused our attention on the existence of two-dimensional signal voltage localized only in one direction of space, that is the propagation direction, it will be interesting to extend this investigation in polar coordinates in order to seek whether a two-dimensional compactlike pulse solitary wave, strictly localized in all directions, could propagate in the two-dimensional electrical network.

APPENDIX: CONSERVED QUANTITY

To justify that (16) is the conserved quantity, let us make in Eq. (14) the change of variables $\eta = aX + bY$, that is $\partial/\partial X = a\partial/\partial\eta$ and $\partial/\partial Y = b\partial/\partial\eta$. By substituting these derivatives into Eq. (14), we obtain the following differential equation:

$$\frac{\partial\phi}{\partial\tau} + \frac{1}{2}\frac{\partial}{\partial\eta}\left[\alpha(av_{p1} + bv_{p2})\phi^2 + (au_{01}\gamma_1 + bu_{02}\gamma_2)\left(\frac{\partial\phi}{\partial\eta}\right)^2\right] = \frac{\epsilon}{2}(au_{01}\lambda_1 + bu_{02}\lambda_2)\frac{\partial^2\phi}{\partial\eta^2}. \tag{A1}$$

Integrating this equation, taking into account that ϕ is localized in a finite region of space, the last two terms of the above equation vanish, which lead to $\frac{\partial}{\partial\tau}\int\phi\,d\eta = 0$, meaning that (16) is time independent and consequently is the conserved quantity.

[1] A. Trombettoni and A. Smerzi, Phys. Rev. Lett. **86**, 2353 (2001).
[2] N. N. Rosanov and G. V. Khodova, J. Opt. Soc. Am. B **7**, 1057 (1990); N. N. Akhmediev, V. V. Afanasjev, and J. M. Soto-Crespo, Phys. Rev. E **53**, 1190 (1996).
[3] R. Hirota and K. Suzuki, J. Phys. Soc. Jpn. **28**, 1366 (1970); Proc. IEEE **61**, 1483 (1973).
[4] P. Rosenau and J. M. Hyman, Phys. Rev. Lett. **70**, 564 (1993); P. Rosenau, *ibid.* **73**, 1737 (1994).
[5] A. Ludu and J. P. Draayer, Physica D **123**, 82 (1998).
[6] R. H. J. Grimshaw, L. A. Ostrovsky, V. I. Shrira, and Y. A. Stepanyants, Surv. Geophys. **19**, 289 (1998).
[7] S. Takeno, Phys. Lett. A **339**, 352 (2005).
[8] P. Rosenau and A. Pikovsky, Phys. Rev. Lett. **94**, 174102 (2005).
[9] A. Pikovsky and P. Rosenau, Physica D **218**, 56 (2006).
[10] D. Takahashi and J. Satsuma, J. Phys. Soc. Jpn. **57**, 417 (1988).
[11] G. Simpson, M. I. Weinstein, and P. Rosenau, Disc. Cont. Dynam. Syst. B **10**, 903 (2008).
[12] P. Rosenau, J. M. Hyman, and M. Staley, Phys. Rev. Lett. **98**, 024101 (2007).
[13] J. Ogasawara and K. Narahara, Prog. Electromagn. Res. Lett. **22**, 29 (2011).

[14] G. Monti and L. Tarricone, Microw. Opt. Technol. Lett. **51**, 2627 (2009).
[15] J. S. Gómez-Diaz, S. Gupta, A. Álvarez-Melcón, and C. Caloz, IEEE Trans. Antennas Propag. **57**, 4010 (2009).
[16] F. G. Gharakhili, M. Shahabadi, and M. Hakkak, Prog. Electromagn. Res. **96**, 237 (2009).
[17] J. Ogasawara and K. Narahara, IEICE Electron. Express **6**, 1576 (2009).
[18] K. Iyer and G. Eleftheriades, IEEE Trans. Antennas Propag. **57**, 1720 (2009).
[19] E. Afshari, H. S. Bhat, A. Hajimiri, and J. E. Marsden, J. Appl. Phys. **99**, 054901 (2006).
[20] K. Narahara and M. Nakamura, Jpn. J. Appl. Phys. **42**, 6327 (2003).
[21] K. Narahara, Prog. Electromagn. Res. Lett. **16**, 69 (2010).
[22] K. Narahara, Jpn. J. Appl. Phys. **42**, 5508 (2003).
[23] F. Kenmogne, D. Yemele, and P. Woafo, Phys. Rev. E **85**, 056606 (2012).
[24] J. C. Comte and P. Marquié, Chaos Solitons Fractals **29**, 307 (2006).
[25] D. Yemélé and F. Kenmogne, Phys. Lett. A **373**, 3801 (2009).
[26] F. Kenmogne and D. Yemélé, Chaos Solitons Fractals **45**, 21 (2012).
[27] D. Ndjanfang, D. Yemélé, P. Marquié, and T. C. Kofané, Prog. Electromagn. Res. B **52**, 207 (2013).
[28] M. Toda, *Theory of Nonlinear Lattice* (Springer, Berlin, 1978).
[29] C. G. Lange and A. C. Newell, SIAM J. Appl. Math. **27**, 441 (1974).
[30] A. K. Jiotsa and T. C. Kofane, J. Phys. Soc. Jpn. **72**, 1800 (2003).
[31] A. Hasegawa and W. F. Brinkman, IEEE J. Quantum Electron. **16**, 694 (1980).
[32] K. Tai, A. Hasegawa, and A. Tomita, Phys. Rev. Lett. **56**, 135 (1986).
[33] M. Antonova and A. Biswas, Commun. Nonlin. Sci. Numer. Simul. **14**, 734 (2009).
[34] S. A. El-Wakil and M. A. Abdou, Chaos Solitons Fractals **31**, 840 (2007).
[35] W. Malfliet and W. Hereman, Phys. Scr. **54**, 563 (1996).
[36] M. Y. Moghaddam, A. Asgari, and H. Yazdani, Appl. Math. Comput. **210**, 422 (2009).
[37] E. Fan and H. Zhang, Phys. Lett. A **246**, 403 (1998).
[38] R. Hirota, *The Direct Method in Soliton Theory* (Cambridge University Press, Cambridge, UK, 2004).
[39] A. V. Porubov, *Amplification of Nonlinear Strain Waves in Solids* (Springer, Berlin, 1978).
[40] F. Kenmogne and D. Yemélé, Phys. Rev. E **88**, 043204 (2013).
[41] F. Rus and F. R. Villatoro, J. Comput. Phys. **228**, 4291 (2009).